

The violent white dwarf merger scenario for the progenitors of Type Ia supernovae

D.-D. Liu,^{1,2,3★} B. Wang,^{1,2★} Ph. Podsiadlowski^{4★} and Z. Han^{1,2}

¹Yunnan Observatories, Chinese Academy of Sciences, Kunming 650216, China

²Key Laboratory for the Structure and Evolution of Celestial Objects, Chinese Academy of Sciences, Kunming 650216, China

³University of Chinese Academy of Sciences, Beijing 100049, China

⁴Department of Astronomy, Oxford University, Oxford OX1 3RH, UK

Accepted 2016 June 29. Received 2016 June 27; in original form 2016 March 28

ABSTRACT

Recent observations suggest that some Type Ia supernovae (SNe Ia) originate from the merging of two carbon–oxygen white dwarfs (CO WDs). Meanwhile, recent hydrodynamical simulations have indicated that the accretion-induced collapse may be avoided under certain conditions when double WDs merge violently. However, the properties of SNe Ia from this violent merger scenario are highly dependent on a particular mass-accretion stage, the so-called WD + He subgiant channel, during which the primary WD is able to increase its mass by accreting He-rich material from an He subgiant before the systems evolves into a double WD system. In this paper, we aim to study this particular evolutionary stage systematically and give the properties of violent WD mergers. By employing the Eggleton stellar evolution code, we followed a large number of binary calculations and obtained the regions in parameter space for producing violent mergers based on the WD + He subgiant channel. According to these simulations, we found that the primary WDs can increase their mass by $\sim 0.10\text{--}0.45 M_{\odot}$ during the mass-accretion stage. We then conducted a series of binary population synthesis calculations and found that the Galactic SN Ia birthrate from this channel is about $0.01\text{--}0.4 \times 10^{-3} \text{ yr}^{-1}$. This suggests that the violent WD mergers from this channel may only contribute to $\sim 0.3\text{--}10$ per cent of all SNe Ia in our Galaxy. The delay times of violent WD mergers from this channel are ≥ 1.7 Gyr, contributing to the SNe Ia in old populations. We also found that the WD + He subgiant channel is the dominant way for producing violent WD mergers that may be able to eventually explode as SNe Ia.

Key words: binaries: close – stars: evolution – supernovae: general – white dwarfs.

1 INTRODUCTION

Type Ia supernovae (SNe Ia), which are defined as SN explosions without H and He lines but with strong Si II absorption lines in their spectra, have been successfully used as standard distance indicators in cosmological studies of dark energy (e.g. Riess et al. 1998; Perlmutter et al. 1999). There is a theoretical consensus that SNe Ia result from thermonuclear explosions of carbon–oxygen white dwarfs (CO WDs) in close binaries (Hoyel & Fowler 1960). According to the nature of the mass donor, two widely accepted models have been proposed, i.e. the single-degenerate (SD) model (e.g. Whelan & Iben 1973; Hachisu, Kato & Nomoto 1996; Li & van den Heuvel 1997; Langer et al. 2000; Han & Podsiadlowski 2004; Meng, Chen

& Han 2009) and the double-degenerate (DD) model (e.g. Iben & Tutukov 1984; Webbink 1984; Nelemans et al. 2001; Toonen, Nelemans & Portegies 2012). The difference between these two models is whether the mass donor is a non-degenerate star (a main-sequence star, a red-giant star or a helium star; the SD model) or another WD merging with the primary WD (the DD model). However, there is still no conclusive evidence to support any progenitor models of SNe Ia. Recent studies suggested that more than one progenitor models may be required to reproduce the observational diversities of SNe Ia (see Podsiadlowski et al. 2008; Howell 2011; Wang & Han 2012; Maoz, Mannucci & Nelemans 2014).

Some recent observations seem to favour the DD model: for example, the lack of H and He lines in the nebular spectra of most SNe Ia (e.g. Leonard 2007; Ganeshalingam, Li & Filippenko 2011), no conclusive proof for the existence of surviving companions (e.g. Badenes et al. 2007; Graham et al. 2015), the lack of radio emission (e.g. Hancock, Gaensler & Murphy 2011; Horesh et al. 2012) and

★ E-mail: liudongdong@ynao.ac.cn (D-DL); wangbo@ynao.ac.cn (BW); podsi@astro.ox.ac.uk (PP)

the observed evidence for the existence of some superluminous events (e.g. Howell et al. 2006; Hicken et al. 2007; Scalzo et al. 2010).¹ Meanwhile, the delay times of SNe Ia, defined as the time interval from the star formation to the thermonuclear explosion, provide an important observational constraint for SN Ia progenitor models. Recent observations have suggested that the delay time distributions (DTDs) of SNe Ia follow a power-law distribution $\sim t^{-1}$ (Totani et al. 2008; Graur et al. 2011; Maoz et al. 2011; Barbary et al. 2012; Sand et al. 2012), which is consistent with the results predicted by the DD model (e.g. Ruiter, Belczynski & Fryer 2009; Mennekens et al. 2010). In addition, Dan et al. (2015) compared the nucleosynthetic yields of thermonuclear explosions from WD mergers with the observations and found that some of their models are good candidates for Type Ia events. Moreover, many double WDs have been proposed as possible progenitor candidates of SNe Ia, e.g. KPD 1930 + 2752, WD 2020–425, V458 Vulpeculae, SBS 1150 + 599A and GD687, etc (Maxted, Marsh & North 2000; Geier et al. 2007, 2010; Napiwotzki et al. 2007; Rodríguez-Gil et al. 2010; Tovmassian et al. 2010).

However, previous studies reveal that the outcome of double WD mergers may be a neutron star resulting from an accretion-induced collapse, rather than a thermonuclear explosion (e.g. Nomoto & Iben 1985; Saio & Nomoto 1985; Timmes, Woosley & Taam 1994). These arguments are based on the assumption that the merging remnant consists of a hot envelope or a thick disc, or even both upon the primary WD (e.g. Kashyap et al. 2015). In that case, the accretion rate from the envelope or disc may be relatively high, leading to the formation of an oxygen–neon (ONe) WD that would collapse into a neutron star when it approaches the Chandrasekhar limit (Nomoto & Iben 1985; Saio & Nomoto 1998). We note that Yoon, Podsiadlowski & Rosswog (2007) argued that the accretion-induced collapse can be avoided for a certain range of parameters and found that they would explode as an SN Ia some 10^5 yr after the initial dynamical merger when considering the rotation of the WDs.

Recently, Pakmor et al. (2010) proposed a new explosion scenario for SNe Ia that are produced by the merging of double WDs referred to as the violent merger scenario. In this scenario, a prompt detonation is triggered while the merger is still ongoing, giving rise to an SN Ia explosion (see also Pakmor et al. 2011, 2012). Pakmor et al. (2010) found that the violent merger of double WDs with almost equal masses of $0.9 M_{\odot}$ can provide an explanation for the formation of subluminal 1991bg-like events. Pakmor et al. (2011) suggested that the minimum critical mass ratio for double WD mergers to produce SNe Ia is about 0.8. Röpke et al. (2012) recently argued that the violent merger model can reproduce the observational properties of SN 2011fe. Additionally, this scenario may also explain the formation of some super-Chandrasekhar mass SNe Ia (e.g. Cody et al. 2014; Moll et al. 2014). For a series of recent theoretical and observational studies of the violent merger scenario see Taubenberger et al. (2013), Kromer et al. (2013), Fesen, Höflich & Hamilton (2015), Seitzzahl et al. (2015), Tanikawa et al. (2015), Chakraborti, Childs & Soderberg (2016) and Bulla et al. (2016).

Ruiter et al. (2013) recently investigated the distribution of the SN Ia brightness based on the violent merger scenario and argued that the theoretical peak-magnitude distribution from their calculations can roughly reproduce their observed properties. The distribution

they obtained depends critically on a particular binary evolutionary stage called the WD + He subgiant channel, during which the primary WD is able to grow in mass by accreting He-rich material from their He companion before eventually evolving into a double WD system. However, this mass-accretion process is still poorly studied, which may influence the binary population synthesis (BPS) results of SNe Ia based on the violent merger scenario (see Ruiter et al. 2013).

In this paper, we systematically study the WD + He subgiant channel for producing SNe Ia via the violent WD merger scenario and obtain the parameter space for the progenitors of SNe Ia. We then present a series of BPS simulations using this parameter space. In Section 2, we describe our methods for the binary evolution calculations and give the main results. The methods and results of our BPS simulations are presented in Section 3. A detailed discussion is provided in Section 4 and finally a summary is given in Section 5.

2 BINARY EVOLUTION CALCULATIONS

2.1 Criteria for violent mergers of double WDs

We conducted a number of binary evolution simulations of WD + He star systems in which the He star fills its Roche lobe at the He main-sequence (MS) or subgiant stage and transfers He-rich material on to the WD. The accreted He-rich material is burned into C and O on the surface of the primary WD, leading to an increase in mass of the WD. When the He shell in the He subgiant donor is exhausted, a double WD system is produced. Subsequently, the double WD system loses its orbital angular momentum and eventually merges due to gravitational wave radiation. We assume that an SN Ia explosion occurs via the violent merger scenario if a double WD system satisfies the following criteria.

- (1) The critical mass ratio of the double WDs, $q_{\text{cr}} = M_{\text{WD2}}/M_{\text{WD1}}$, is larger than 0.8, where M_{WD1} and M_{WD2} are the mass of the massive WD and the less massive WD, respectively (see Pakmor et al. 2011).
- (2) The mass of the massive WD in the double WD system is larger than $0.8 M_{\odot}$ (see Pakmor et al. 2010; Sim et al. 2010; Ruiter et al. 2013).
- (3) The delay times (t) of SNe Ia are shorter than the Hubble time. In this paper, the delay time of SNe Ia is defined as

$$t = t_{\text{evol}} + t_{\text{acc}} + t_{\text{GW}}, \quad (1)$$

where t_{evol} , t_{acc} and t_{GW} are the evolutionary time-scale from the primordial binaries to the formation of the WD + He star systems, the evolutionary time-scale from the formation of the WD + He star systems to the formation of double WDs, and the merging time-scale of double WDs, respectively. Here, t_{GW} is defined as the time-scale for the double WDs to be brought together and eventually merge through gravitational wave radiation (e.g. Landau & Lifshitz 1971):

$$t_{\text{GW}} = 8 \times 10^7 \times \frac{(M_{\text{WD1}} + M_{\text{WD2}})^{1/3}}{M_{\text{WD1}} M_{\text{WD2}}} P^{8/3}, \quad (2)$$

where P is the orbital period of the WD binary in hours, t_{GW} is in unit of years, M_{WD1} and M_{WD2} are in unit of M_{\odot} .

2.2 Binary evolution code

We employed the Eggleton stellar evolution code (Eggleton 1973; Han, Podsiadlowski & Eggleton 1994; Pols et al. 1995, 1998; Eggleton & Kiseleva-Eggleton 2002) to simulate the evolution of

¹ Some of these observed clues may also be explained by the SD model after considering the spin-up/spin-down processes of WDs (e.g. Di Stefano, Voss & Claeys 2011; Justham 2011; Hachisu, Kato & Nomoto 2012; Wang et al. 2014).

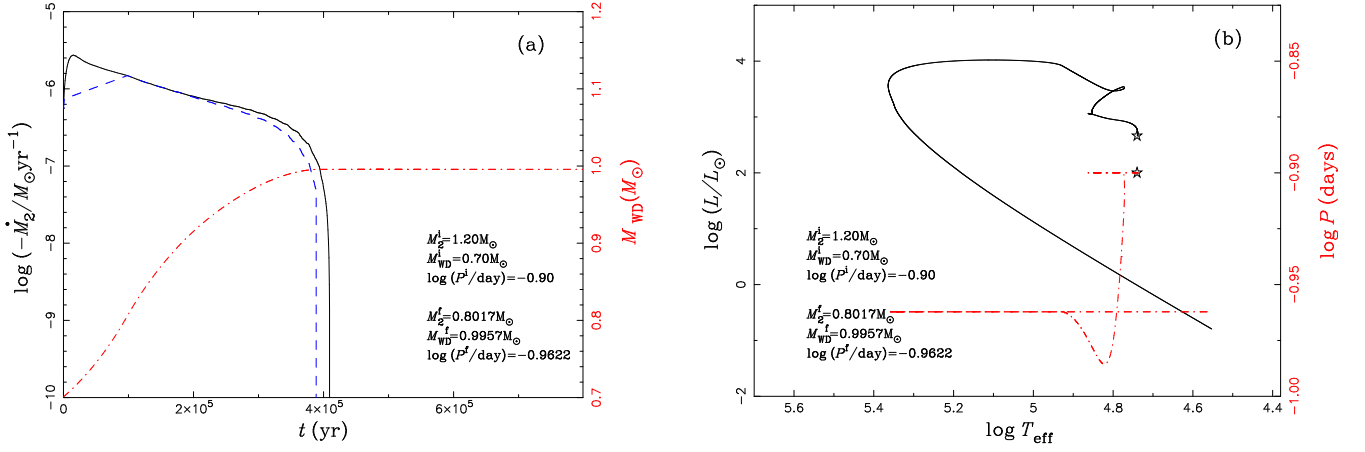


Figure 1. A representative example of binary evolution calculations that can produce an SN Ia through the violent merger scenario, in which the He star first fills its Roche lobe at the subgiant stage. Panel (a): the evolution of the mass-transfer rate (solid curve), the WD mass-growth rate (dashed curve) and the WD mass (dash-dotted curve) as a function of time for the binary calculation. Panel (b): the luminosity of the mass donor (solid curve) and the binary orbital period (dash-dotted curve) as a function of effective temperature. Asterisks in the right-hand panel indicate the position where the simulation starts. The initial binary parameters of WD + He star system and the parameters of the double WD systems at its formation time are also given in these two panels.

WD + He star systems up to beginning of the merger phase. The initial setup and physical assumptions in this code are similar to those in Wang et al. (2009). We assumed that the He star models have a helium mass fraction $Y = 0.98$ and metallicity $Z = 0.02$. The process of Roche lobe overflow (RLOF) is calculated using the boundary condition

$$\dot{M}_2 = C \max \left[0, \left(\frac{r_{\text{star}}}{r_{\text{lobe}}} - 1 \right)^3 \right], \quad (3)$$

where \dot{M}_2 is the mass-transfer rate, r_{star} is the radius of the star that fills its Roche lobe, r_{lobe} is the radius of its Roche lobe and C is a constant (see Han, Tout & Eggleton 2000). Here, we set $C = 1000 M_{\odot} \text{ yr}^{-1}$, assuming that the lobe-filling star overflows the Roche lobe stably and as necessary, but never too much, i.e. $(r_{\text{star}}/r_{\text{lobe}} - 1) \leq 0.001$.

According to WD models computed with constant mass-accretion rates, Nomoto (1982) provided a critical mass-transfer rate written as

$$\dot{M}_{\text{cr}} = 7.2 \times 10^{-6} (M_{\text{WD}}/M_{\odot} - 0.6) M_{\odot} \text{ yr}^{-1}. \quad (4)$$

We utilized the optically thick wind model when the mass-transfer rate \dot{M}_2 is larger than \dot{M}_{cr} (Kato & Hachisu 1994; Hachisu et al. 1996). In this case, we assume that the accreted He-rich material is burned into C and O stably at the rate of \dot{M}_{cr} , and that the unprocessed material is blown away from the binary in the form of an optically thick wind. When $\dot{M}_{\text{st}} < \dot{M}_2 < \dot{M}_{\text{cr}}$, we assume that the He shell burns stably at the rate of \dot{M}_2 and that no stellar wind is triggered, where \dot{M}_{st} is the minimum accretion rate for stable He shell burning (see Kato & Hachisu 2004). When $\dot{M}_2 < \dot{M}_{\text{st}}$, the prescription of Kato & Hachisu (2004) is adopted for the mass accumulation process during He shell flashes on the surface of the WD. During this He shell flash process, the mass increase rate of the WD, \dot{M}_{WD} , is calculated as

$$\dot{M}_{\text{WD}} = \eta_{\text{He}} \dot{M}_2, \quad (5)$$

where η_{He} is the mass accumulation efficiency for He shell burning.

We added the prescriptions above in the Eggleton stellar evolution code and followed the evolution of WD + He star systems. We assume that the mass lost from these systems takes away the specific

orbital angular momentum of the accreting WD. In this work, we simulated the evolution of about 800 WD + He star systems. The range of initial masses of the WDs (M_{WD}^i) is $0.65\text{--}1.07 M_{\odot}$; the upper mass limit, $1.07 M_{\odot}$, is the maximum mass for a single CO WDs based on standard stellar models (see Iben & Tutukov 1985; Umeda et al. 1999). The range of the initial masses of the He stars (M_{He}^i) is $0.8\text{--}2.6 M_{\odot}$, and the range of the initial orbital periods of the binaries (P^i) is $0.04\text{--}0.50$ d. We produced a large and dense model grid, which can be employed in Monte Carlo BPS simulations.

2.3 The evolution of typical WD + He star systems

In Figs 1 and 2, we present a representative and an extreme example for the binary evolution producing SNe Ia based on the violent merger scenario. In each of these two figures, panel (a) shows the \dot{M}_{He} , \dot{M}_{WD} and M_{WD} as a function of time, and panel (b) presents the evolutionary tracks of the He stars in the Hertzsprung–Russell diagram and the evolution of the orbital periods.

Fig. 1 shows a representative example for the evolution of a WD + He star system in which the He star first fills its Roche lobe when it has evolved to the subgiant stage. In this case the initial binary parameters are $(M_{\text{WD}}^i, M_{\text{He}}^i, \log P^i) = (0.7, 1.2, -0.9)$, where M_{WD}^i and M_{He}^i are in units of M_{\odot} , and P^i is in units of days. When the He star evolves to the subgiant stage, it expands quickly and soon fills its Roche lobe, leading to a mass-transfer phase. At the beginning, the mass-transfer rate exceeds the critical rate \dot{M}_{cr} and enters a stellar wind stage. At this stage, part of the transferred He-rich material burns into C and O and accumulates on the surface of the WD, while the unprocessed part is blown away from the binary in the form of an optically thick wind. After about 1×10^5 yr, the mass-transfer rate drops below \dot{M}_{cr} and the optically thick wind stops. The mass-transfer rate continues to decrease and drops below \dot{M}_{st} after about 1×10^5 yr. In this case, the system is in a weak He shell flash stage and the WD still grows in mass. After about 2×10^5 yr, the envelope of the He star is exhausted and eventually a WD is produced. When the double WDs are formed, the final mass of the primary WD is $M_{\text{WD}}^f = 0.9957 M_{\odot}$, the mass of the WD produced from the He star is $M_{\text{He}}^f = 0.8017 M_{\odot}$, and the period of the WD binary is $\log(P^f \text{ d}^{-1}) = -0.9622$. The double WDs will merge in

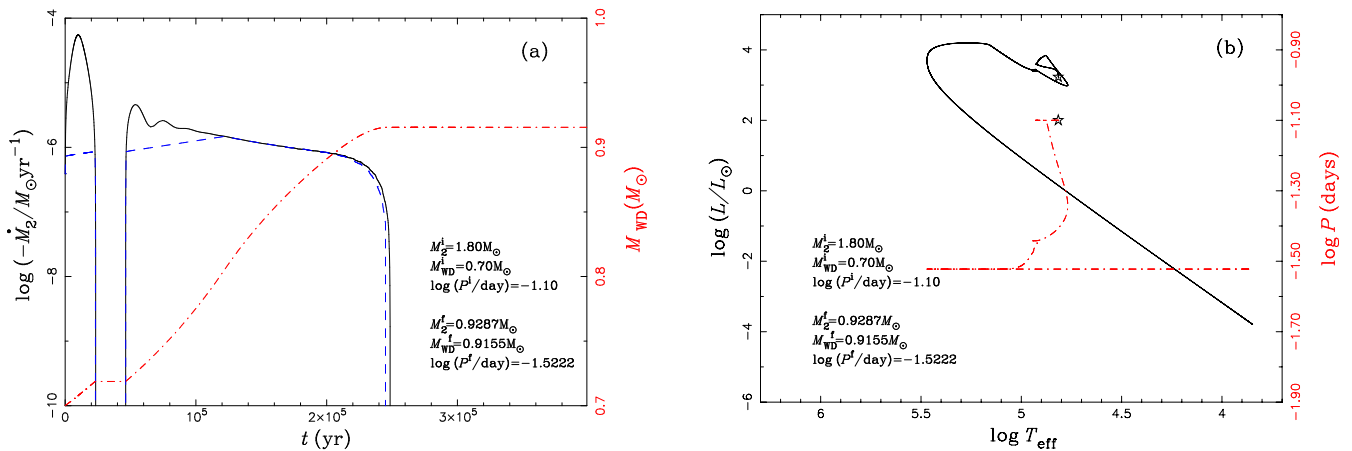


Figure 2. Similar to Fig. 1, but for an extreme case in which the He star first fills its Roche lobe in the He main-sequence stage and again at the subgiant stage.

about 1.6 Gyr after their formation, which is driven by gravitational wave radiation.

Fig. 2 presents an extreme case in which the He star first fills its Roche lobe at the He MS stage and again at the He subgiant stage. In this case, the initial binary parameters are $(M_{\text{WD}}^i, M_2^i, \log P^i) = (0.7, 1.8, -1.1)$. Since this binary has a short orbital period, the He star first fills its Roche lobe at its MS stage, resulting in a stable mass-transfer process. At this stage, \dot{M}_2 is larger than \dot{M}_{cr} , triggering the optically thick wind. After about 2.2×10^4 yr, the He star shrinks below its Roche lobe, and mass transfer stops. After about 2.0×10^4 yr, the central He in the He star is exhausted, and a CO core is formed. The He star then expands and fills its Roche lobe again. The subsequent evolution of this binary is similar to the case presented in Fig. 1. When the two WDs are form: $M_{\text{WD}}^f = 0.9155 M_\odot$, $M_2^f = 0.9287 M_\odot$ and $\log(P^f \text{ d}^{-1}) = -1.5222$. The double WDs will merge in about 48 Myr after their formation due to gravitational wave radiation.

2.4 Initial parameters for violent mergers of double WDs

By calculating the evolution of a large number of WD + He star systems, we obtained a large and dense model grid. In Figs 3–6, we present the final outcomes of the binary evolution calculations in the initial orbital period–secondary mass ($\log P^i - M_2^i$) plane. In these figures, the initial masses of the primordial WDs range from 0.65 to $1.07 M_\odot$. The filled circles represent WD + He star systems which can explode as SNe Ia in their future evolution based on the violent merger scenario. We also present the contours of initial parameters for producing SNe Ia in these figures and found that the primary WDs may increase their mass by about $0.10 - 0.45 M_\odot$ by accretion from the He donors. According to these figures, the initial masses of He stars (M_2^i) range from 0.9 to $2.2 M_\odot$ and the initial periods of the binaries (P^i) range from 1.2 to 12 h for producing SNe Ia. For a larger metallicity, we expect that the grids will move to larger initial He-star masses and larger initial orbital periods, which leads to earlier SN Ia explosions (e.g. Wang & Han 2010).

The WD + He star systems in Figs 3–6 denoted by crosses, pluses and triangles will evolve to double WDs that do not satisfy all the criteria for violent mergers presented in Section 2.1; i.e. these systems will fail to produce SNe Ia via the violent merger scenario. Among these binaries represented by crosses (in the upper-right regions) fail to form SNe Ia as the WDs resulting from the He donors are too massive, leading to the mass ratios (q) less than 0.8;

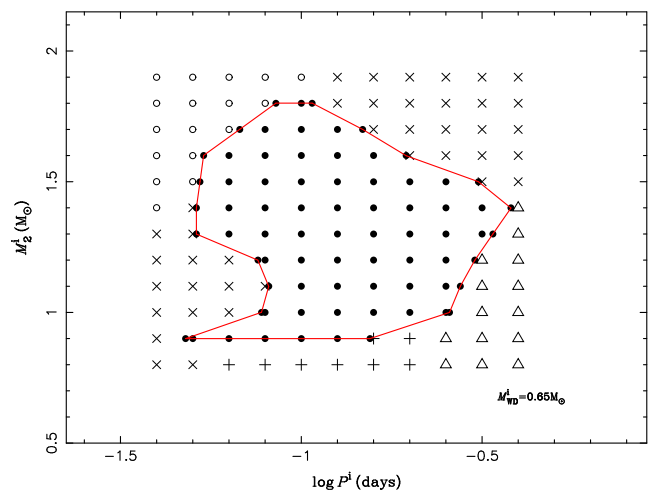


Figure 3. Final results of the binary evolution calculations in the initial orbital period–secondary mass ($\log P^i, M_2^i$) plane of WD + He star systems for an initial WD mass of $0.65 M_\odot$. The filled circles denote the binaries which can produce violent WD mergers and eventually produce SN Ia explosions. The plus signs, crosses and triangles indicate that the formed double WD systems do not satisfy all the criteria for violent mergers presented in Section 2.1. The open circles represent binaries which would enter a CE stage during the mass-transfer phase.

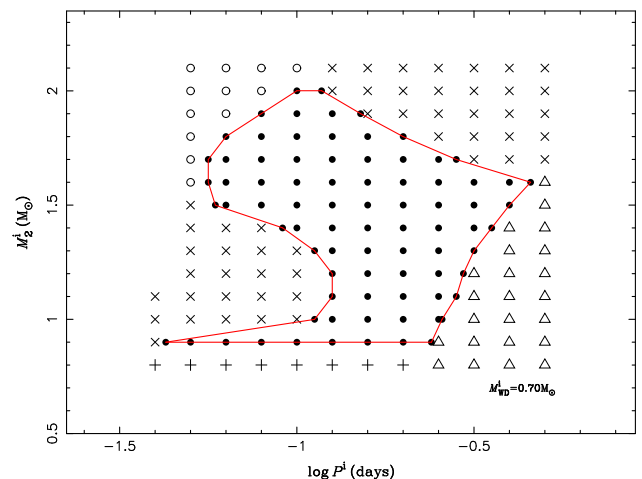


Figure 4. Similar to Fig. 3, but for an initial WD mass of $0.7 M_\odot$.

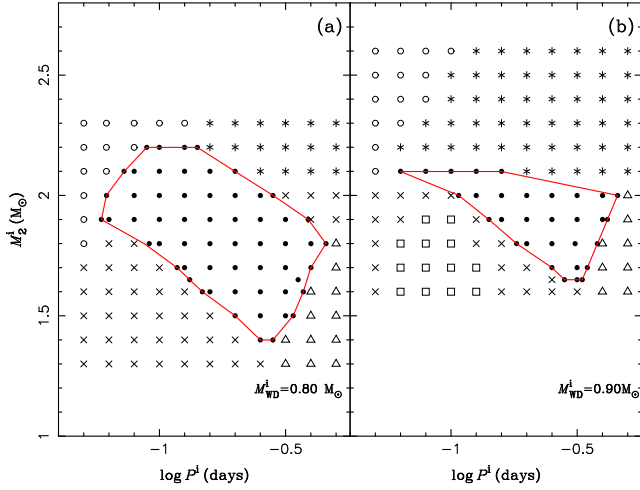


Figure 5. Similar to Fig. 3, but for initial WD masses of 0.8 and 0.9 M_{\odot} . The snowflakes represent the binaries in which the He subgiants would evolve to ONe WDs but not CO WDs, and the squares denote the binaries that can produce SNe Ia through the Chandrasekhar mass SD model (Wang et al. 2009).

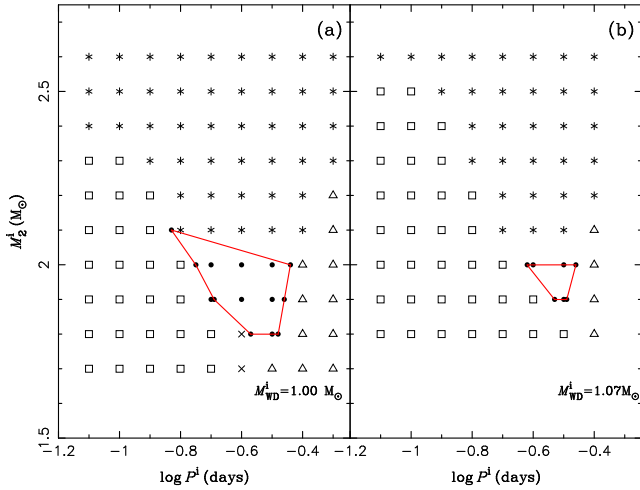


Figure 6. Similar to Fig. 3, but for initial WD masses of 1.0 and 1.07 M_{\odot} .

those in the lower-left regions fail to form SNe Ia as the primary WDs are too massive, resulting in $q < 0.8$. For the binaries denoted by open circles in Figs 3–5, mass transfer is dynamically unstable when the He subgiants fill their Roche lobe, leading to a common envelope (CE) stage. These binaries may also evolve to double WDs and produce SNe Ia through the violent merger scenario, which will be discussed further in Section 3. Massive He stars in binaries marked by snowflakes will evolve to ONe WDs but not CO WDs; the outcome of the merger of CO WD + ONe WD systems may be a hybrid SN, in which the ONe core may collapse and CO upon the surface may detonate (see Dan et al. 2014). The primary WDs in binaries indicated by squares will increase their mass to the Chandrasekhar limit and explode as SNe Ia before the He stars evolve to the WD stage (see Wang et al. 2009).

In Fig. 7, we show the regions in the parameter space of WD + He star systems which can lead to SNe Ia via violent mergers with various initial WD masses (i.e. $M_{\text{WD}}^i = 0.65, 0.7, 0.8, 0.9, 1.0$ and $1.07 M_{\odot}$). In this figure, it is obvious that the contours for producing violent WD mergers move to the upper-right region as the initial

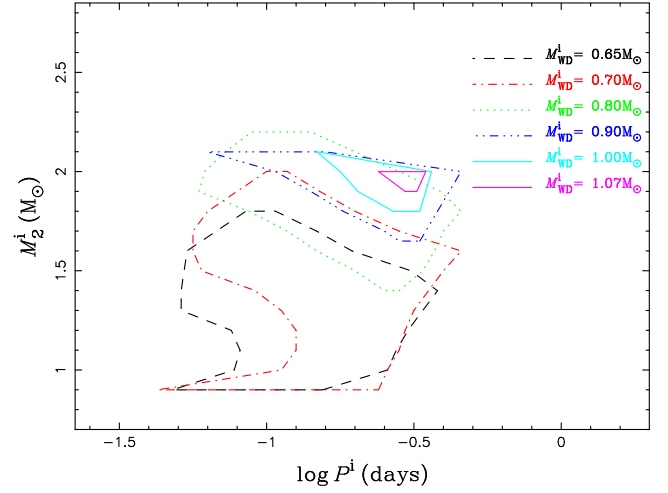


Figure 7. Regions in the orbital period–secondary mass ($\log P^i - M_2^i$) plane for WD + He star systems which can produce SNe Ia for various initial WD masses.

WD mass increases, which follows from the requirement of a large mass ratio ($q > 0.8$). Massive He stars tend to form massive WDs, and large orbital periods result in little material being transferred from the He stars to the WDs. Thus, for the binaries with massive He donors and large periods in the upper right region, the WDs evolved from He stars could be massive enough to merge violently with the primary WDs as the initial mass of the WDs increases.

3 BINARY POPULATION SYNTHESIS

3.1 BPS methods

BPS, which is to follow the evolution of millions of primordial binaries, is an important method to obtain the birthrates and delay times of SNe Ia (e.g. Han 1998; Yungelson & Livio 1998; Nelemans et al. 2001). We performed a series of BPS Monte Carlo simulations to investigate the properties of the violent mergers. We assume that an SN Ia explosion would occur if the initial parameters of a WD + He star system are located in the contours of the $\log P^i - M_2^i$ plane for the specific M_{WD}^i . The properties of the double WDs at the moment of their formation are investigated by interpolations in the three-dimensional grid ($M_{\text{WD}}^i, M_2^i, \log P^i$) of the WD + He star systems calculated in Section 2. Employing the rapid binary evolution code developed by Hurley, Tout & Pols (2002), we simulated the evolution of binaries from their formation to the formation of WD + He star systems with a metallicity $Z = 0.02$. In each simulation, 4×10^7 primordial binary samples are included.

The basic assumptions and initial parameters in our Monte Carlo simulations are described in the following.

- (1) We employed the initial mass function of Miller & Scalo (1979) for the distribution of the primordial primary mass (M_1).
- (2) For the primordial secondary mass (M_2), we take a constant mass ratio ($q' = M_1/M_2$) distribution, i.e. $n(q') = 1$.
- (3) All stars are considered to be members of binaries with circular orbits.
- (4) The distribution of initial orbital separations is assumed to be constant in $\log a$ for wide binaries and falls off smoothly for

close binaries, where a is orbital separation (Han, Tout & Eggleton 1995):

$$an(a) = \begin{cases} \alpha_{\text{set}}, & a_0 < a < a_1, \\ \alpha_{\text{set}}(a/a_0)^m, & a \leq a_0, \end{cases} \quad (6)$$

where $\alpha_{\text{set}} \approx 0.07$, $m \approx 1.2$, $a_0 = 10 R_\odot$ and $a_1 = 5.75 \times 10^6 R_\odot$. This distribution of orbital separations implies that about 50 per cent of stellar systems have orbital periods less than 100 yr, and that there is an equal number of wide binary systems per logarithmic interval.

We simply employed a constant star formation rate (SFR) to provide a rough description of spiral galaxies, or alternatively, a delta-function SFR (i.e. a single starburst) to approximate elliptical galaxies (or star clusters). For the case of a constant SFR, the SFR is calibrated by assuming that a binary with its primary mass larger than $0.8 M_\odot$ is formed per year (see Iben & Tutukov 1984; Han et al. 1995; Hurley et al. 2002). From this calibration, an SFR of $5 M_\odot \text{ yr}^{-1}$ over the past 15 Gyr is obtained (see also Willems & Kolb 2004), which is similar to the situation of our Galaxy (Yungelson & Livio 1998; Han & Podsiadlowski 2004). For the case of a delta-function SFR, a burst producing $10^{10} M_\odot$ in stars is adopted.

The WD + He star systems originate from CE evolution (see Section 3.2). However, the process of CE interaction is still unclear (e.g. Ivanova et al. 2013). The CE interaction is usually parametrized based on the relationship between the orbital energy and the binding energy. We adopted the standard energy prescription to calculate the output of the CE stage (see Webbink 1984). There exist two uncertain parameters for this prescription, i.e. the CE ejection efficiency (α_{CE}) and a stellar structure parameter (λ). The value of λ depends on the structure and evolutionary phase of the mass donor. For simplicity, we combined α_{CE} and λ as a single free parameter (i.e. $\alpha_{\text{CE}}\lambda$) to describe the process of the CE ejection, and set $\alpha_{\text{CE}}\lambda = 0.5, 1.0$ and 1.5 to examine its influence on the final results.

3.2 Binary evolutionary channels

There are two evolutionary channels that can produce WD + He star systems and then form SNe Ia depending on the evolutionary phase of the primordial primary when the primordial secondary has evolved to the He-star phase (see Fig. 8):

Channel A. The primordial primary first fills its Roche lobe when it has evolved to the subgiant stage, resulting in a stable mass-transfer process. At the end of RLOF, the primary becomes a He star. Subsequently, the secondary evolves to the subgiant stage and fills its Roche lobe. This mass-transfer phase is dynamically unstable, leading to a CE process. If the CE can be ejected, the secondary turns into an He star, and the primary evolves to the He subgiant stage. The primary soon fills its Roche lobe again and transfers He-rich material stably on to the surface of the secondary. After mass transfer, the He shell of the primary will be exhausted, and a WD + He star system will be produced. The following evolution of the binary is similar to that presented in Figs 1 and 2 and an SN Ia would eventually be produced via the violent merger scenario. For this channel, the primordial binaries are in the range of $M_{1,i} \sim 4.0\text{--}5.5 M_\odot$, $M_{2,i} \sim 2.5\text{--}4.5 M_\odot$ and $P^i \sim 5\text{--}330$ d.

Channel B. The evolution of this channel is similar to that of Channel A before the primary evolves to be a He star. The primary then continues to evolve and will fill its Roche lobe again when it has evolved to the He subgiant stage. At this stage, the primary transfers its He-rich envelope stably to the secondary, leading to the forma-

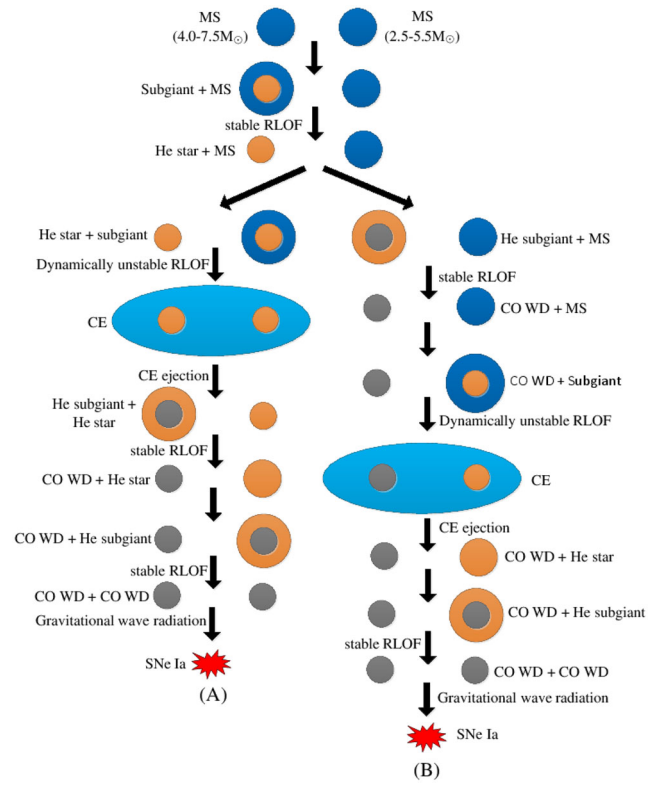


Figure 8. Binary evolutionary channels for producing SNe Ia from the violent merger scenario.

Table 1. The birthrates and delay times of SNe Ia for three simulation sets based on the violent merger scenario.

Set	$\alpha_{\text{CE}}\lambda$	$\nu(10^{-3} \text{ yr}^{-3})$	DTDs(Gyr)
1	0.5	0.01	2.69–8.71
2	1.0	0.19	>2.14
3	1.5	0.40	>1.70

Note. ν and DTDs are the birthrates and the delay time distributions of SNe Ia, respectively.

tion of a WD + MS star system. After that, the secondary continues to evolve and will fill its Roche lobe at the subgiant stage. At this stage, a CE may be formed due to dynamically unstable mass transfer. If the CE is ejected, a WD + He star system could eventually be formed. The subsequent evolution of the binary is similar to that presented in Figs 1 and 2. For this channel, the primordial binaries are in the range of $M_{1,i} \sim 4.5\text{--}7 M_\odot$, $M_{2,i} \sim 2.5\text{--}5 M_\odot$ and $P^i \sim 3\text{--}23$ d.

3.3 BPS results

3.3.1 Birthrates and delay times of SNe Ia

By performing a series of BPS Monte Carlo simulations, we obtained the birthrates and delay times of SNe Ia for the violent merger scenario (see Table 1). We found that the masses of the primordial primaries range from $4.0\text{--}7.5 M_\odot$, the masses of the primordial secondaries from 2.5 to $5.5 M_\odot$, and the primordial orbital periods are in the range of $3\text{--}347$ d for producing SNe Ia based on the WD + He subgiant channel. When these binaries evolve to become WD + He star systems, the masses of the WDs are in the range of

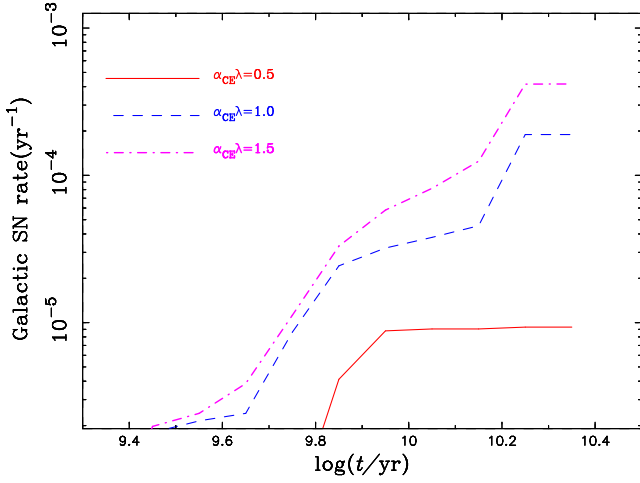


Figure 9. Evolution of Galactic SN Ia birthrates with time for a constant Population I SFR ($Z = 0.02$, $\text{SFR} = 5 \text{ M}_\odot \text{ yr}^{-1}$) based on the WD + He subgiant channel. The solid, dashed and dash-dotted curves show the results of different CE ejection parameters with $\alpha_{\text{CE}}\lambda = 0.5$, 1.0 and 1.5, respectively.

$0.65\text{--}1.07 \text{ M}_\odot$, the masses of the He stars range from 0.9 to 2.1 M_\odot and the orbital periods are from 1.2 to 10.6 h.

Fig. 9 represents the evolution of the Galactic birthrate of SNe Ia as a function of time for a constant SFR of $5 \text{ M}_\odot \text{ yr}^{-1}$. This leads to a Galactic SN Ia birthrate for the violent merger scenario of $\sim 0.01\text{--}0.4 \times 10^{-3} \text{ yr}^{-1}$ based on the WD + He subgiant channel. For comparison, the observed Galactic SN Ia birthrate is $\sim 3\text{--}4 \times 10^{-3} \text{ yr}^{-1}$ (e.g. Cappellaro & Turatto 1997). The violent merger scenario studied here may thus contribute $\sim 0.3\text{--}10$ per cent of all SNe Ia in our Galaxy. Thus, we suggest that this scenario is a subchannel for producing SNe Ia. We also note that the SN Ia birthrate increases with the value of $\alpha_{\text{CE}}\lambda$. The reason is that, for a larger value of $\alpha_{\text{CE}}\lambda$, CE ejection will require less orbital energy, making it easier to form WD + He star systems that are located in the correct region for producing SNe Ia.

In Fig. 10, we show the DTDs for violent mergers from the WD + He subgiant channel (see thick lines). These distributions are obtained based on the assumption of a single starburst producing 10^{10} M_\odot in stars. The delay times of SNe Ia from the WD + He subgiant channel range from ~ 1.7 Gyr to the Hubble time. Here, the minimum delay time of 1.7 Gyr comes from the left boundary of the grids for producing SNe Ia shown in Fig. 7. We also note that, if we dropped the mass ratio constraint, it could be expected that the left boundary of the grids for producing SNe Ia in Fig. 7 would move to the left, which would lead to a smaller minimum delay time. We suggest that the violent merger scenario from this channel may contribute to SNe Ia with long delay times. We also found that the gravitational wave radiation time-scale t_{GW} plays the dominant role in these long delay times. It is worth noting that there is a real cut-off in $\log(t)$ at large times for the case with $\alpha_{\text{CE}}\lambda = 0.5$, while the cut-off is artificial for the other cases as the system ages have already reached the Hubble time.

We also note that the DTDs do not obey a t^{-1} relation. There are two reasons for this, as follows. (i) For the grids in Fig. 7, the parameter space for producing violent mergers increases as the orbital period increases, leading to more binary systems with large orbital periods that can produce SNe Ia. (ii) The CE ejection process tends to form binaries with long orbital periods. Since the delay time in this scenario is sensitive to the orbital period, a binary with long

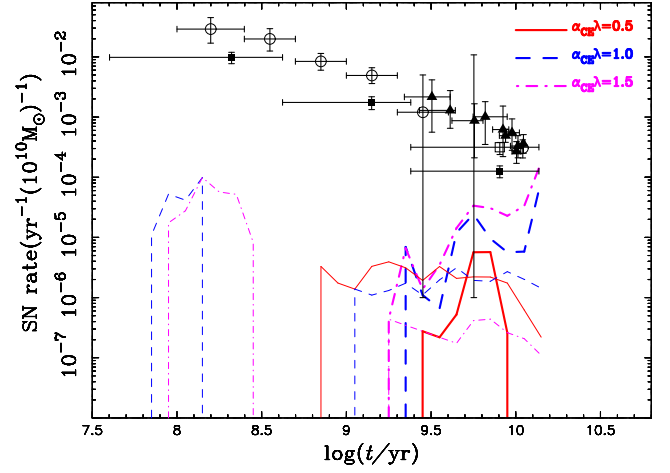


Figure 10. DTDs of SNe Ia based on the violent merger scenario. The thick curves show the DTDs of violent mergers from the WD + He subgiant channel, while the thin curves represent the cases from other channels. The open circles are from Totani et al. (2008), the filled triangles, squares are taken from Maoz, Keren & Avishay (2010) and Maoz, Mannucci & Timothy (2012) and the open square is from Graur & Maoz (2013).

orbital period will have a long gravitational wave radiation time, leading to a long delay time.

Aside from the WD + He subgiant channel, there are other channels to form violent mergers (e.g. Ruiter et al. 2011). Those other channels can also produce violent mergers without going through the particular mass-accretion process that is so important in this paper (for details see Meng et al. 2011). Using our BPS code, we also simulated these other channels for producing SNe Ia via the violent merger scenario. We found that the Galactic violent merger rate from these channels is about $0.7\text{--}1.8 \times 10^{-5} \text{ yr}^{-1}$, which is quite low. The contribution of violent mergers from these channels is less than 1 per cent of all SNe Ia (see also Meng et al. 2011). In Fig. 10, we also present the DTDs of violent mergers from these other formation channels (thin curves). The figure shows that the SN Ia delay times from the violent merger scenario range from 70 Myr to the Hubble time; violent mergers from the WD + He subgiant channel mainly contribute to SNe Ia in old populations, while violent mergers from other channels contribute to SNe Ia in young populations.

3.3.2 Mass distributions of double WDs

We calculated the properties of the double WDs from the WD + He subgiant channel by adopting interpolations in the three-dimensional grid ($M_{\text{WD}}^i, M_2^i, \log P^i$) obtained in Section 2. We found that the periods of double WDs range from 1.5 to 7.5 h at the beginning of their formation. Fig. 11 shows the density distribution of violent merger WDs in the $M_{\text{WD}}^f - M_2^f$ plane. In this simulation, 4×10^7 primordial sample binaries are included and the CE ejection parameter $\alpha_{\text{CE}}\lambda$ is set to be 1.5. This distribution shows that, in most cases, M_{WD}^f is larger than M_2^f , while the fraction with $M_2^f > M_{\text{WD}}^f$ is only ~ 7 per cent. We also note that the masses of the WDs formed from the primordial primaries can be as large as 1.3 M_\odot , which is due to the accretion of He-rich material from the He donors on to the WDs with lower masses.

In Fig. 12, we present the initial mass distribution and the final mass distribution of the primary WDs with $\alpha_{\text{CE}}\lambda = 1.0$. The initial masses of the primary WDs range from 0.65 to 1.07 M_\odot ,

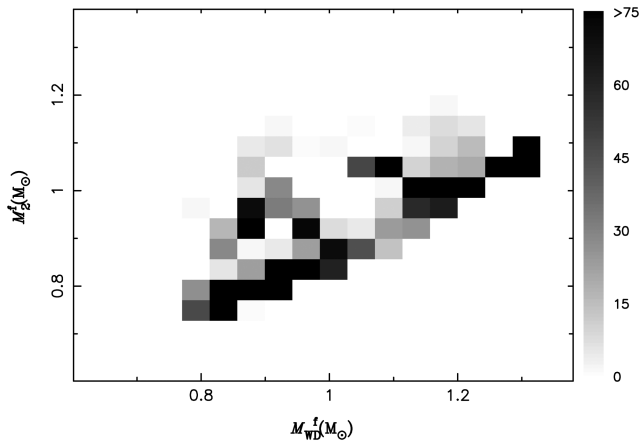


Figure 11. The density distribution of violent mergers from the WD + He subgiant channel in the $M_{\text{WD}}^f - M_2^f$ plane, where M_{WD}^f and M_2^f are the final mass of the primary WD and the mass of the WD produced from the He star, respectively. Here, we have set $\alpha_{\text{CE}}\lambda = 1.5$.

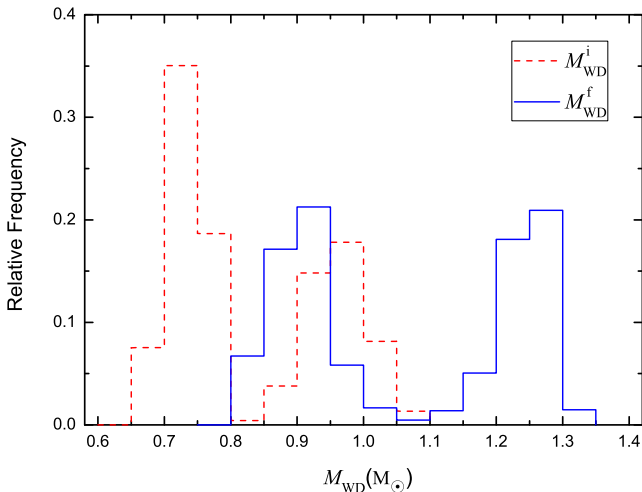


Figure 12. Distribution of the initial/final masses of the primary WDs with $\alpha_{\text{CE}}\lambda = 1.0$, in which M_{WD}^i is the initial mass of the primary WDs (red dashed line), and M_{WD}^f is the final mass of the primary WDs (blue solid line).

while the final masses are in the range of $0.8\text{--}1.35 M_{\odot}$. Note that there are two peaks for these distributions. The left peak of initial masses is about $0.7 M_{\odot}$, while the right peak is around $0.95 M_{\odot}$; for the final mass distribution, the left peak is about $0.9 M_{\odot}$ and the right peak is near the $1.25 M_{\odot}$. Fig. 13 shows the total mass distribution of the violent WD mergers for different values of $\alpha_{\text{CE}}\lambda$. The total masses are in the range of $1.4\text{--}2.4 M_{\odot}$. We note that there are also two peaks in these three distributions. The left peaks are around $1.7 M_{\odot}$ and the right ones are about $2.2 M_{\odot}$. These two peaks originate from two different formation channels. The left peaks mainly originate from *Channel A*, while the right ones are mainly from *Channel B* (see Section 3.1); the primordial binaries in *Channel B* have slightly massive primordial primaries and significantly shorter periods, resulting in the formation of more massive primary WDs.

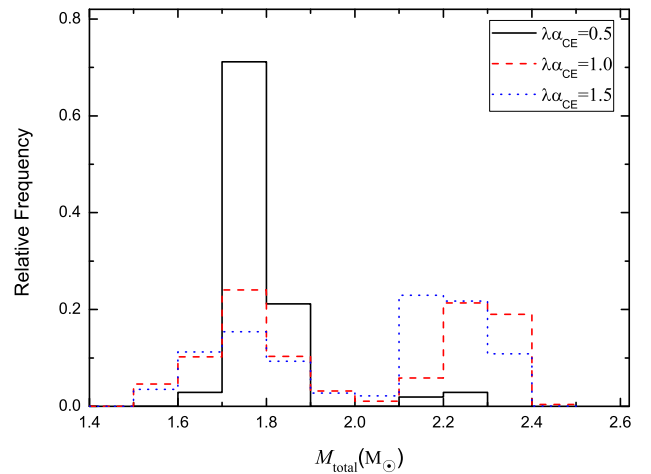


Figure 13. Distribution of the total mass of double WDs with different values of $\alpha_{\text{CE}}\lambda$. The black solid, red dashed and blue dotted lines represent the cases with $\alpha_{\text{CE}}\lambda = 0.5, 1.0$ and 1.5 , respectively.

4 DISCUSSION

For the violent merger scenario, the mass-accretion process during which the primary WD accretes material from an He subgiant is crucial for the production of SNe Ia. By considering an identical value of α_{CE} as Ruiter et al. (2013), i.e. $\alpha_{\text{CE}}\lambda = 0.5$ in this paper, we found that such a particular mass-accretion stage can be expected to occur in about 43.7 per cent of all the binary systems which would eventually contribute to SNe Ia; this is consistent with the fraction given by Ruiter et al. (2013). For other cases with larger $\alpha_{\text{CE}}\lambda$, this fraction would be much higher in our simulations: 91.8 per cent for the case of $\alpha_{\text{CE}}\lambda = 1.0$ and 85.7 per cent for the case of $\alpha_{\text{CE}}\lambda = 1.5$. Thus, we suggest that the WD + He subgiant channel may be the dominant way for producing violent mergers of double WDs that can form SNe Ia. During the mass-accretion stage, the primary WDs can increase their mass by about $0.1\text{--}0.45 M_{\odot}$ from the He donors based on our calculations, which is slightly wider than the mass range ($\sim 0.15\text{--}0.35 M_{\odot}$) presented by Ruiter et al. (2013). This is due to the fact that we employed full stellar evolution calculations, while Ruiter et al. (2013) adopted a simple analytical fitting formula for estimating the mass-accretion rate. We compared our prescriptions with Ruiter et al. (2013) by calculating the evolution of a WD + He star system provided in Section 2.3 of Ruiter et al. (2013). This system has a $0.84 M_{\odot}$ WD and a $1.25 M_{\odot}$ He star separated by $1.73 R_{\odot}$. Our calculation shows that $M_{\text{WD}}^f = 1.2 M_{\odot}$ and $M_2^f = 0.84 M_{\odot}$, compared to $M_{\text{WD}}^f = 1.19 M_{\odot}$ and $M_2^f = 0.77 M_{\odot}$ in Ruiter et al. (2013). When this double WDs is formed, their separation is $1.74 R_{\odot}$ for our calculation and $1.92 R_{\odot}$ for Ruiter et al. (2013).

In addition, Ruiter et al. (2013) claimed that the DTDs from violent mergers agree rather well with observations and that the violent merger scenario may be the dominant contributor to SNe Ia in field galaxies. They argued that violent mergers from the WD + He subgiant channel may contribute to SNe Ia with delay times > 150 Myr, a conclusion that is quite different from our results. This is caused by the different criteria for the critical mass ratio for double WDs between Ruiter et al. (2013) and this work. We note that Ruiter et al. (2013) used a relatively weak criterion with $\eta = 1.5$ for the critical mass ratio (q_{cr}) of the WD binaries to calculate the SN Ia birthrate and DTD (see formula 1 in their paper). From fig. 5 of Ruiter et al. (2013), one can see that the difference between their

q -cut (with $\eta = 1.5$) and no q -cut at all is very minor, especially for the massive WDs of double WDs at the high-mass end, which means that the double WDs with nearly all mass ratios are thought to be able to produce SNe Ia in the Ruiter et al. (2013) estimates.

The brightness of SN Ia explosions originating from violent mergers are mainly determined by the final mass of the massive WDs (M_{WD1}). The reason is that the less massive WD is totally destroyed in the merging process and that almost all of the iron-group elements (including ^{56}Ni) are produced in the thermonuclear explosion inside the massive WD. For the violent mergers with low-mass WDs ($M_{\text{WD1}} < 1.1 M_{\odot}$), their low density causes incomplete silicon burning during the explosion, resulting in a lower yield of ^{56}Ni compared with normal SNe Ia, corresponding to subluminal SNe Ia (e.g. Pakmor et al. 2010, 2011). However, for the violent mergers with massive WDs ($M_{\text{WD1}} > 1.1 M_{\odot}$), the yields of these massive mergers are still quite uncertain, and they are potential candidates for explaining super-Chandrasekhar mass SNe Ia (Cody et al. 2014; Moll et al. 2014).

However, the minimum critical mass ratio of double WDs to produce prompt detonations and SNe Ia through the violent merger scenario is still quite uncertain (e.g. Pakmor et al. 2011; Sato et al. 2016). In this work, we adopted $q_{\text{cr}} \geq 0.8$, which is consistent with Pakmor et al. (2011), but somewhat optimistic. If a larger critical mass ratio (e.g. $q_{\text{cr}} \geq 0.9$) for the double WDs is adopted, the contribution of violent mergers to the Galactic birthrate of SNe Ia would be $\sim 0.1\text{--}1.1 \times 10^{-4} \text{ yr}^{-1}$, accounting for only 0.2–3 per cent of all SNe Ia in the Galaxy, and the delay times of SNe Ia would be larger than 3.5 Gyr. Furthermore, Sato et al. (2015) argued that an SN Ia would be produced during the merging process if the masses of both WDs are in the range of $0.9 M_{\odot} \leq M_{\text{WD}} \leq 1.1 M_{\odot}$, whereas the thermonuclear explosion can be expected in the stationary rotating merger remnant stage if the massive WDs in double WD systems are in the mass range of $0.7 M_{\odot} \leq M_{\text{WD}} \leq 0.9 M_{\odot}$ and the total masses are larger than the Chandrasekhar mass (see also Cody et al. 2014; Moll et al. 2014). Chen et al. (2012) also claimed that the SN Ia birthrate from the DD model may decrease significantly when considering different constraints for double WDs. We note that recent studies suggested that a thin He shell on the surface of CO WDs could potentially produce SNe Ia more easily in WD mergers (e.g. Dan et al. 2012; Pakmor et al. 2013).

Furthermore, the merging of CO WD + He WD systems may also contribute to the birthrates of SNe Ia based on the double-detonation scenario (see Dan et al. 2012; Pakmor et al. 2013). In this scenario, mass transfer is relatively unstable and occurs within the direct impact regime, in which Kelvin–Helmholtz instabilities may trigger an explosion of the He shell on the surface of the CO WD (see Guillochon et al. 2010). The shock compression in the CO core caused by the He explosion could potentially lead to the explosion of the whole WD. Less ^{56}Ni would be produced during the thermonuclear explosions as the accretors always have sub-Chandrasekhar masses; the SNe Ia resulting from such mergers may have lower luminosities than normal SN Ia explosions, i.e. they may contribute to the class of subluminal SNe Ia (e.g. Sim et al. 2010; Dan et al. 2012). Considering the possibility of CO WD + He WD systems for producing subluminal SNe Ia, future BPS studies are needed to explore the properties of SNe Ia through the CO WD + He WD scenario.

5 SUMMARY

In this paper, we employed the Eggleton stellar evolution code to simulate the evolution of WD + He star systems until the onset of

the merging of double WDs, including the effect of an optically thick wind. With these simulations, we obtained the regions in parameter space for producing SNe Ia via the violent merger scenario for different initial WD masses. Using the results from these binary evolution calculations, we performed a series of BPS Monte Carlo simulations and obtained the Galactic birthrates and DTDs of SNe Ia. Aside from the WD + He subgiant channel, we also obtained the BPS results of violent mergers from other formation channels. We found that the WD + He subgiant channel is the dominant contributor of violent mergers and that the overall SN Ia birthrate from the violent merger scenario accounts for at most 10 per cent of the inferred observational results in our Galaxy. SNe Ia from the violent merger scenario mainly contribute to SNe Ia with long delay times based on the WD + He subgiant channel studied here. We note that the SN Ia progenitor survey (SPY) performed by the European Southern Observatory was designed to search for double WDs (Napiwotzki et al. 2004; Nelemans et al. 2005; Geier et al. 2007). The double WDs formed from the WD + He subgiant channel have He-rich atmospheres, which means that those binaries should be double DB WDs. In order to put further constraints on the violent merger scenario, large samples of observed double DB WDs are needed. Additionally, more numerical simulations related to the violent WD merger scenario are required to constrain the properties of the resulting SNe Ia.

ACKNOWLEDGEMENTS

We acknowledge useful comments and suggestions from the referee. We acknowledge Stephen Justham, Xuefei Chen and Xiangcun Meng for their helpful discussions. This work is supported by the National Basic Research Program of China (973 programme, 2014CB845700), the National Natural Science Foundation of China (Nos 11322327, 11390374 and 11521303), the Chinese Academy of Sciences (Nos KJZD-EW-M06-01 and XDB09010202), the Natural Science Foundation of Yunnan Province (Nos 2013HB097, 2013FB083 and 2013HA005), and the Youth Innovation Promotion Association CAS.

REFERENCES

- Badenes C., Hughes J. P., Bravo E., Langer N., 2007, *ApJ*, 662, 472
- Barbary K. et al., 2012, *ApJ*, 745, 32
- Bulla M., Sim S. A., Pakmor R., Kromer M., Taubenberger S., Röpke F. K., Hillebrandt W., Seitenzahl I. R., 2016, *MNRAS*, 455, 1060
- Cappellaro E., Turatto M., 1997, in Ruiz-Lapuente P., Cannal R., Isern J., eds, *Thermonuclear Supernovae*. Kluwer, Dordrecht, p. 77
- Chakraborti S., Childs F., Soderberg A., 2016, *ApJ*, 819, 37
- Chen X., Jeffery C. S., Zhang X., Han Z., 2012, *ApJ*, 755, L9
- Cody R. et al., 2014, *ApJ*, 788, 75
- Dan M., Rosswog S., Guillochon J., Ramirez-Ruiz E., 2012, *MNRAS*, 422, 2417
- Dan M., Rosswog S., Brüggen M., Podsiadlowski P., 2014, *MNRAS*, 438, 14
- Dan M., Guillochon J., Brüggen M., Ramirez-Ruiz E., Rosswog S., 2015, *MNRAS*, 454, 4411
- Di Stefano R., Voss R., Claeys J. S. W., 2011, *ApJ*, 738, L1
- Eggleton P. P., 1973, *MNRAS*, 163, 279
- Eggleton P. P., Kiseleva-Eggleton L., 2002, *ApJ*, 575, 461
- Fesen R. A., Höflich P. A., Hamilton A. J. S., 2015, *ApJ*, 804, 140
- Ganeshalingam M., Li W., Filippenko A. V., 2011, *MNRAS*, 416, 2607
- Geier S., Nesslering S., Heber U., Przybilla N., Napiwotzki R., Kudritzki R. P., 2007, *A&A*, 464, 299
- Geier S., Heber U., Kupfer T., Napiwotzki R., 2010, *A&A*, 515, A37
- Graham M. L., Nugent P. E., Sullivan M., Filippenko A. V., Cenko S. B., Silverman J. M., Clubb K. I., Zheng W., 2015, *MNRAS*, 454, 1948

- Graur O., Maoz D., 2013, *MNRAS*, 430, 1746
- Graur O. et al., 2011, *MNRAS*, 417, 916
- Guillochon J., Dan M., Ramirez-Ruiz E., Rosswog S., 2010, *ApJ*, 709, L64
- Hachisu I., Kato M., Nomoto K., 1996, *ApJ*, 470, L97
- Hachisu I., Kato M., Nomoto K., 2012, *ApJ*, 756, L4
- Han Z., 1998, *MNRAS*, 296, 1019
- Han Z., Podsiadlowski Ph., 2004, *MNRAS*, 350, 1301
- Han Z., Podsiadlowski Ph., Eggleton P. P., 1994, *MNRAS*, 270, 121
- Han Z., Podsiadlowski Ph., Eggleton P. P., 1995, *MNRAS*, 272, 800
- Han Z., Tout C. A., Eggleton P. P., 2000, *MNRAS*, 319, 215
- Hancock P. P., Gaensler B. M., Murphy T., 2011, *ApJ*, 735, L35
- Hichen M., Garnavich P. M., Prieto J. L., Blondin S., DePoy D. L., Kirshner R. P., Parrent J., 2007, *ApJ*, 669, L17
- Horesh A. et al., 2012, *ApJ*, 746, 21
- Howell D. A., 2011, *Nature Commun.*, 2, 350
- Howell D. A. et al., 2006, *Nature*, 443, 308
- Hoyel F., Fowler W. A., 1960, *ApJ*, 132, 565
- Hurley J. R., Tout C. A., Pols O. R., 2002, *MNRAS*, 329, 897
- Iben I., Tutukov A. V., 1984, *ApJS*, 54, 335
- Iben I., Tutukov A. V., 1985, *ApJS*, 58, 661
- Ivanova N., Justham S., Avendano Nandez J. L., Lombardi J. C., 2013, *Science*, 339, 433
- Justham S., 2011, *ApJ*, 730, L34
- Kashyap R., Fisher R., García-Berro E., Aznar-Siguán G., Ji S., Lorén-Aguilar P., 2015, *ApJ*, 800, L7
- Kato M., Hachisu I., 1994, *ApJ*, 437, 802
- Kato M., Hachisu I., 2004, *ApJ*, 613, L129
- Kromer M. et al., 2013, *ApJ*, 778, L18
- Landau L. D., Lifshitz E. M., 1971, *Classical Theory of Fields*. Pergamon Press, Oxford
- Langer N., Deutschmann A., Wellstein S., Höflich P., 2000, *A&A*, 362, 1046
- Leonard D. C., 2007, *ApJ*, 670, 1275
- Li X.-D., van den Heuvel E. P. J., 1997, *A&A*, 322, L9
- Maoz D., Keren S., Avishay G.-Y., 2010, *ApJ*, 722, 1879
- Maoz D., Mannucci F., Li W., Filippenko A. V., Della Valle M., Panagia N., 2011, *MNRAS*, 412, 1508
- Maoz D., Mannucci F., Timothy D. B., 2012, *MNRAS*, 426, 3282
- Maoz D., Mannucci F., Nelemans G., 2014, *ARA&A*, 52, 107
- Maxted P. F. L., Marsh T. R., North R. C., 2000, *MNRAS*, 317, L41
- Meng X., Chen X., Han Z., 2009, *MNRAS*, 395, 2103
- Meng X., Chen W., Yang W., Li Z., 2011, *A&A*, 525, A129
- Mennekens N., Vanbeveren D., De Greve J. P., De Donder E., 2010, *A&A*, 515, A89
- Miller G. E., Scalo J. M., 1979, *ApJS*, 41, 513
- Moll R., Raskin C., Kasen D., Woosley S. E., 2014, *ApJ*, 785, 105
- Napiwotzki R. et al., 2004, in Hilditch R. W., Hensberge H., Pavlovski K., eds, *ASP Conf. Ser. Vol. 318, Spectroscopically and Spatially Resolving the Components of the Close Binary Stars*. Astron. Soc. Pac., San Francisco, p. 402
- Napiwotzki R. et al., 2007, in Napiwotzki R., Burleigh M. R., eds, *ASP Conf. Ser. Vol. 372, Binary White Dwarfs in the Supernova Ia Progenitor Survey*. Astron. Soc. Pac., San Francisco, p. 387
- Nelemans G., Yungelson L. R., Portegies Zwart S. F., Verbunt F., 2001, *A&A*, 365, 491
- Nelemans G. et al., 2005, *A&A*, 440, 1087
- Nomoto K., 1982, *ApJ*, 253, 798
- Nomoto K., Iben I., 1985, *ApJ*, 297, 531
- Pakmor R., Kromer M., Röpke F. K., Sim S. A., Ruiter A. J., Hillebrandt W., 2010, *Nature*, 463, 61
- Pakmor R., Hachinger S., Röpke F. K., Hillebrandt W., 2011, *A&A*, 528, A117
- Pakmor R., Kromer M., Taubenberger S., Sim S. A., Röpke F. K., Hillebrandt W., 2012, *ApJ*, 747, L10
- Pakmor R., Kromer M., Taubenberger S., Springel V., 2013, *ApJ*, 770, L8
- Perlmutter S. et al., 1999, *ApJ*, 517, 565
- Podsiadlowski Ph., Mazzali P., Lesaffre P., Han Z., Förster F., 2008, *New Astron. Rev.*, 52, 381
- Pols O. R., Tout C. A., Eggleton P. P., Han Z., 1995, *MNRAS*, 274, 964
- Pols O. R., Schröder K. P., Hurly J. R., Tout C. A., Eggleton P. P., 1998, *MNRAS*, 298, 525
- Riess A. et al., 1998, *AJ*, 116, 1009
- Rodríguez-Gil P. et al., 2010, *MNRAS*, 407, L21
- Röpke F. K. et al., 2012, *ApJ*, 750, L19
- Ruiter A. J., Belczynski K., Fryer C., 2009, *ApJ*, 699, 2026
- Ruiter A. J., Belczynski K., Sim S. A., Hillebrandt W., Fryer C. L., Fink M., Kromer M., 2011, *MNRAS*, 417, 408
- Ruiter A. J. et al., 2013, *MNRAS*, 429, 1425
- Saio H., Nomoto K., 1985, *A&A*, 150, 21
- Saio H., Nomoto K., 1998, *ApJ*, 500, 388
- Sand D. J. et al., 2012, *ApJ*, 746, 163
- Sato Y., Nakasato N., Tanikawa A., Nomoto K., Maeda K., Hachisu I., 2015, *ApJ*, 807, 105
- Sato Y., Nakasato N., Tanikawa A., Nomoto K., Maeda K., Hachisu I., 2016, *ApJ*, 821, 67
- Scalzo R. A. et al., 2010, *ApJ*, 713, 1073
- Seitenzahl I. R. et al., 2015, *MNRAS*, 447, 1484
- Sim S. A., Röpke F. K., Hillebrandt W., Kromer M., Pakmor R., Fink M., Ruiter A. J., Seitenzahl I. R., 2010, *ApJ*, 714, L52
- Tanikawa A., Nakasato N., Sato Y., Nomoto K., Maeda K., Hachisu I., 2015, *ApJ*, 807, 40
- Taubenberger S., Kromer M., Pakmor R., Pignata G., Maeda K., Hachinger S., Leibundgut B., Hillebrandt W., 2013, 775, L43
- Timmes F. X., Woosley S. E., Taam R. E., 1994, *ApJ*, 420, 348
- Toonen S., Nelemans G., Portegies Z. S., 2012, *A&A*, 546, A70
- Totani T., Morokuma T., Oda T., Doi M., Yasuda N., 2008, *PASJ*, 60, 1327
- Tovmassian G. et al., 2010, *ApJ*, 714, 178
- Umeda H., Nomoto K., Yamaoka H., Wanao S., 1999, *ApJ*, 513, 861
- Wang B., Han Z., 2010, *A&A*, 515, A88
- Wang B., Han Z., 2012, *New Astron. Rev.*, 56, 122
- Wang B., Meng X., Chen X., Han Z., 2009, *MNRAS*, 395, 847
- Wang B., Justham S., Liu Z.-W., Zhang J.-J., Liu D.-D., Han Z., 2014, *MNRAS*, 445, 2340
- Webbink R. F., 1984, *ApJ*, 277, 355
- Whelan J., Iben I., 1973, *ApJ*, 186, 1007
- Willems B., Kolb U., 2004, *A&A*, 419, 1057
- Yoon S.-C., Podsiadlowski Ph., Rosswog S., 2007, *MNRAS*, 390, 933
- Yungelson L., Livio M., 1998, *ApJ*, 497, 168

This paper has been typeset from a \LaTeX file prepared by the author.